ISSN: 1304-7981 Number: **12**, Year: **2016**, Pages: **111-125** **http://jnrs.gop.edu.tr**

Gaziosmanpasa University
Graduate School of Natural and Applied Sciences
Journal of New Results in Science

Received: 15.05.2016 *Invited Editor*: Mahmut Hekim
Accepted: 08.09.2016 *Area Editor*: Zafer Dogan

Broken Rotor Bar Fault Diagnosis in Induction Motors using Resampling Based Order Tracking Analysis Method

Tufan DOĞRUER[a,1] (tufan.dogruer@gop.edu.tr)
Mehmet AKAR[b] (mehmet.akar@gop.edu.tr)

[a] *Gaziosmanpaşa University, Department of Electronic and Automation, 60250, Tokat*
[b] *Gaziosmanpaşa University, Department of Mechatronics Engineering, 60250, Tokat*

Abstract – Induction motors are the most popular motors used in the industry because of their simple structure, steadfast operation, and high efficiency. Unexpected failures of these motors reduce the production capacity while increasing the maintenance and expenditure cost. So condition monitoring motors and troubleshooting methods are highly necessary for the electrical motors. In this proposed study, the effect of broken rotor bar faults on motor current signal in three-phased motors was examined under stationary and non-stationary conditions. The proposed method contains clear information about the fault under both operation conditions.

Keywords *-*
Broken rotor bar,
Fault detection
Motor faults.

1. Introduction

Induction motors are the electrical machines that are mostly used in industrial areas. Its main reason is that they are economical and high efficient, they don't need much maintenance because they don't contain brush in their structure, their speed control is easy, and they have a solid structure. Because of it's a critical element in industry, their operation cost increases in case of a failure. They lead to production loss and rise of maintenance cost. So, it has become important today that failures appearing in the electrical motors be diagnosed in advance, and the problem be solved. The date of the failures occurring in the electrical motors is almost equal to the date of the electrical motor. The manufacturers and the users used to assume earlier that the way to protect the electrical motors is to keep them away from over current and voltage [1]. However, fault detection has become difficult with

[1]***Corresponding Author***

the increase of faults that is parallel to the development of electrical motors [2].

The faults occurring in induction motors are related to three main components of the motor. Those are rotor, stator, and bearing. Besides, some of those faults are related to the mechanical and magnetic circuit problems, while some of them occur because of the electrical problems [3]. According to the results of the studies conducted with the help of condition monitoring and imaging techniques, distribution of the faults occurring in induction motors is displayed on Table 1 [4]. In addition, Figure 1 shows the failure of induction motor [5].

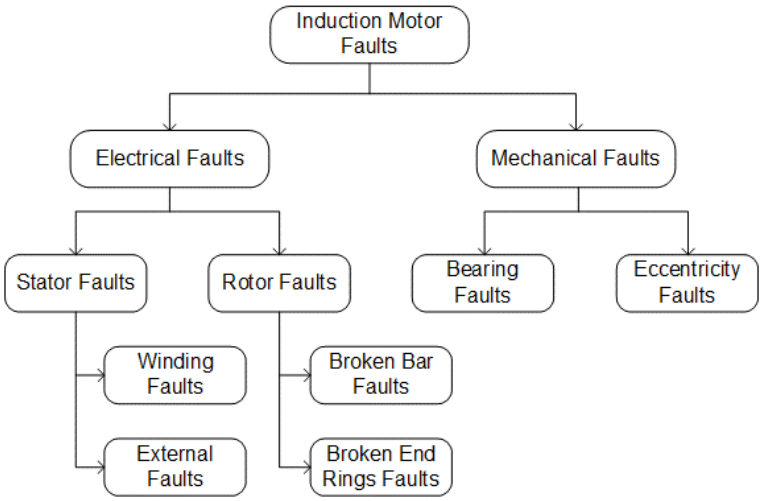

Figure 1. Induction motor fault categories [5]

Bearing faults constitute about 40% of the faults occurring in induction motors. The fault in bearings occur because inner or outer rings, the ball bearings placed between the rings, or the link that connects the ball bearings and that is called as cage fault. Vibration analysis, temperature analysis, and stator currents monitoring technique are used commonly in the detection of those faults.

Table 1. Distribution of faults in induction motors

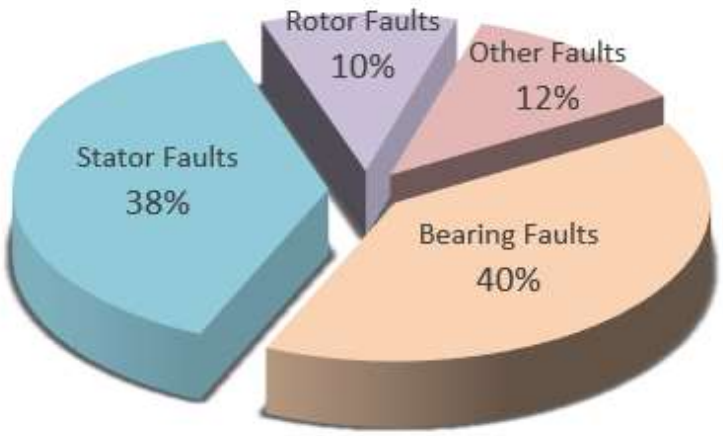

Stator faults are generally related with the insulation breakdowns, and they constitute about 38% of the faults occurring in induction motors. Stator windings contain insulated copper conductors placed in stator slots. Stator winding faults appear as a result of an insulation breakdown between two adjacent windings [4]. Armature and stator insulation can be broken down because of a few reasons. These are high temperature, loosely coupled junctions, defective joints at the end of the windings, fouling due to the lube oil, moisture, and dust, short circuit or motor take-off strength, electrical discharges, and leakages in the cooling system [1].

As seen on Table 1, even though the rotor related faults in induction motors have a 10% percentile, they cause secondary faults in the motor if not detected on time. Therefore, serious breakdowns occur in motor, and they cause the motor stop.

The method that is most widely used for fault detection in induction motors is motor current signal analysis (MCSA). This method is based on the principle of monitoring the frequency components of the monitored signal via FFT analysis. The MCSA method, which gives successful results for stationary signals, is inadequate for non-stationary signals [6].

This proposed study consists of five parts. The first part is the introduction part, and it is about the importance and faults of the induction motors. In the second part, the reasons of broken rotor bars faults, their effects on motor, and the fault detection techniques are mentioned. RB-OTA (Resampling based order tracking analysis) used for detecting the broken rotor bar faults is explained in the third part. In the fourth part, testing apparatus is introduced, and the data acquisition is presented in graphs. The results of the experimental study are given in the fifth part.

2. Induction Motor with Broken Rotor Bar

Induction motors are symmetrical systems. When an induction motor is operated under three phases, a symmetrical and periodical electromagnetic rotary field occurs in the air gap. Under ideal conditions, current, voltage, and magnetic flux distributions are symmetrically. Besides, the faults and defects in induction motors disturb this symmetry. The abnormalities within the rotor structure change the rotor resistance and inductance, and disturb the electrical and magnetic field. As a result, oscillation occurs in stator currents [1].

Squirrel cage rotor type is preferred more for the motors used in industry due to its simple structure and low cost. Over time squirrel cage rotor bar cracking or breaking faults occur in these rotors [7]. Because of various reasons rotor bars may have been broken wholly or partially. These reasons can be listed as; over heat and loss or thermal effects resulting from the sparks, electromagnetic forces, unbalanced magnetic attractions, magnetic effects stemming from the noise and vibration, the effects stemming from the manufacturing defects, the effects stemming from torque, centrifuge, and revolution, chemical effects or environmental effects causing the rotor material wear away because of the moisture, sheet losses, fatigued mechanisms, and the mechanical stress occurring as a result of bearing faults [1].

Several scientific studies have been conducted in order to detect those faults in rotor. The study of detecting the broken rotor bar faults with the help of artificial neural network, which is one of those studies, has been carried out scientifically by Arabacı [8]. The data collected from healthy and faulty motors have been examined in time and frequency domains, and the parts in which the most clear fault signs are observed have been used for Artificial Neural Network Training. As a result, it has been proved scientifically that rotor fault detection in squirrel-cage induction motors can be carried out with motor current analysis [8]. Shuo Chen (2008) has carried out the detection of broken rotor bar fault in induction motors by using Prony analysis technique. An induction motor model with broken rotor bar has been developed using the MATLAB/Simulink program. The results of the simulation and the experimental studies were validated by having been compared to each other [9]. Supangat (2008) has examined the detection of stator and rotor faults (short-circuit winding faults, broken rotor bar faults and eccentricity faults) within the induction motors that operate under various loads by using three types of sensor signals (current, vibration, and magnetic flux) [10]. Mehala et al. (2009), presented a methodology for the detection of broken rotor bar fault of induction motor based on wavelet analysis of the stator current. They achieved good results in the field of fault diagnosis of induction motor using wavelet analysis [11]. Costa et al. (2015), compared two diagnostic methods for the detection of broken bars in induction motors with squirrel-cage type rotors: FFT method and wavelet method. Their main goal is to find out the advantages of wavelet transform method compared to Fourier transform method in rotor failure detection of induction motors [12]. Bayrak et al. (2016), they have developed a new algorithm power-based for detection broken rotor bar. Experimental results have demonstrated that the new algorithm detects the faults more reliable and effective than the other methods [13]. In addition [14-18] can be examined.

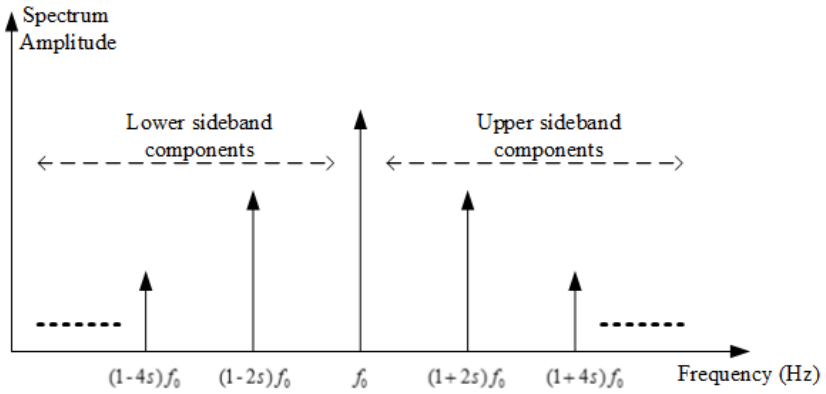

Figure 2. Sideband frequencies around the fundamental line frequency [19]

The effects of broken rotor bar are various. Sidebands arise at the right and left sides of the supply frequency in the fault stator current. The frequency computation of these sidebands is shown in Equation 1 [20]. Figure 2 shows the sideband frequency components specific to a broken rotor bar fault, which is given in (1) for k=1 and 2.

$$f_b = (1 \pm 2ks)f_0 \quad k = 1, 2, 3, \ldots. \tag{1}$$

f_b represents broken rotor bar fault frequency, s represents slip, f_0 represents the supply frequency, and k represents a constant number such as k = 0,1,2,..,n in (1).

The faulty rotors consisting of broken rotor bars have certain disadvantages. Any breakdown in the rotor bars cause secondary faults in induction motors. These breakdowns lead to very serious faults in motor. As the motor efficiency decreases, energy consumption increases. That raises the energy cost in the businesses. For example, the current in the bar that is adjacent to the faulty bar increases at a rate of 50%, and it leads to unbalanced current and torque impulses. So the average torque decreases. If the motor is in a dangerous place, any spark or electric arc at the time that motor starts may cause an unexpected accident. Because current doesn't pass through the broken bar, excess current will pass through the adjacent bars and these bars will overheat. That overheat will damage the insulation and stator windings. Besides, if the broken rotor bar fault expands more, it will finally cause the motor stop [9].

3. Order Tracking Analysis Technique

Order tracking analysis (OTA) is one of the important vibration analysis techniques used for the rotating machines. The advantage of OTA technique computed to the other vibration analysis techniques shows itself in the analysis of non-stationary signals. Within the non-stationary analyses, frequency and amplitude information will change with the rotation of one shaft. Also extra information is necessary in order to obtain successful results from the analysis of non-stationary signals in comparison with the stationary signals. This extra information is the speed information measured from the motor shaft [21]. In recent years, many researchers have examined the different types of OTA. The most frequently used OTA methods can be divided into three categories [21]. The first one of these methods is the Fourier Transform Based OTA (FT-OTA) method which is supported by Blough. This method isn't used in non-stationary signals. It is used for observing the system generally and getting a first impression. The second method is RB-OTA method. This OTA method was first published by Potter and his collogues in 1989. The third method is Vold/Kalman Filter Based OTA method. This method overcomes most of the resolution limits. The biggest difference of this method from the other two methods is that time story of the order can be elicited from the original data together with amplitude and phase information.

3.1. RB-OTA Method

Most of the limits of the Fast Fourier Transform (FFT) based methods are overcome by this method. In this method, constant angular intervals are sampled in constant with the constant sampling time. The time sampled with the constant sampling is transformed into equal angular intervals with the help of interpolation algorithm. The time formed by equal angular intervals is calculated with the operation of the encoder signal. After sampling, it is determined what the counterpart of the data in time domain will be in angular domain [22]. This process can be carried out as real-time with special data collecting equipment systems [6].

The data having been transformed into angular domain is processed according to FFT or discrete time Fourier transform [22]. As long as the transformations occur on the data in angular domain, output spectral lines represent the constant rates. That means that there are equivalent sampling relations in angle/order domain in comparison with the time/frequency sampling relation.

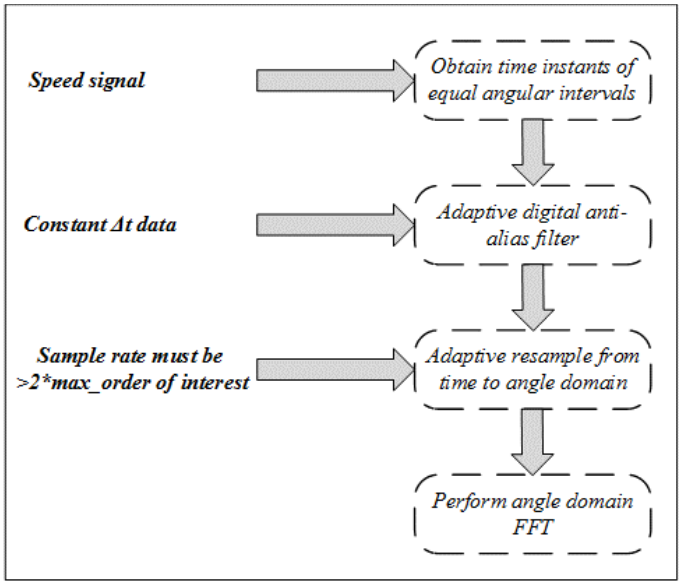

Figure 3. Flow chart of resampling based order tracking process [6]

$$\Delta_0 = \frac{1}{R} = \frac{1}{N * \Delta\theta}$$
$$R = N * \Delta\theta$$
$$O_{nyquist} = O_{\max.} = \frac{O_{sample}}{2} \quad (2)$$
$$O_{sample} = \frac{1}{\Delta\theta}$$

In Equation 2, Δ_0 stands for the order resolution of output order spectrum, R stands for the total number of the values analyzed, N stands for the total number of the time points on the transformations conducted, Δθ stands for the angular interval of the resampled samples, O_sample stands for the angular sample at the time of the data being sampled, O_nyquist stands for Nyquist sample and O_max stands for the maximum sample that can be analyzed.

Sampling relations in Equation 2 share similarities with FFT analysis sampling conditions given in time domain. Order transform is the reverse of the number of transformations having been analyzed. That means that for good order resolution, the analysis should be applied on much resolution. Maximum order that can be analyzed can be found with the number of samples per cycle or angular sampling rate. The angular domain counterparts of the transformations are shown in Equation 3 [22].

$$a_m = \frac{1}{N}\sum_{n=1}^{N} x(n\Delta\theta)\cos(2\pi o_m n\Delta\theta)$$
$$b_m = \frac{1}{N}\sum_{n=1}^{N} x(n\Delta\theta)\sin(2\pi o_m n\Delta\theta) \quad (3)$$

In Equation 3, o_m, a_m and b_m stand respectively for the order that has been analyzed, the Fourier coefficient belonging to Cosine term for o_m, and the Fourier coefficient belonging to Sine term for o_m.

4. Experimental Study

Three-phased induction motor was used in the experimental study. Induction motor used in the experimental study is driven by the inverter. Foucault brake is used in loading the motor. The Foucault brake produces a load torque between 0-20 N.m depending on the voltage applied to its poles and accordingly the current that it draws. Experimental test rig is seen on Figure 4. Additionally the tag values related to motor and Foucault brake are presented in Table 2.

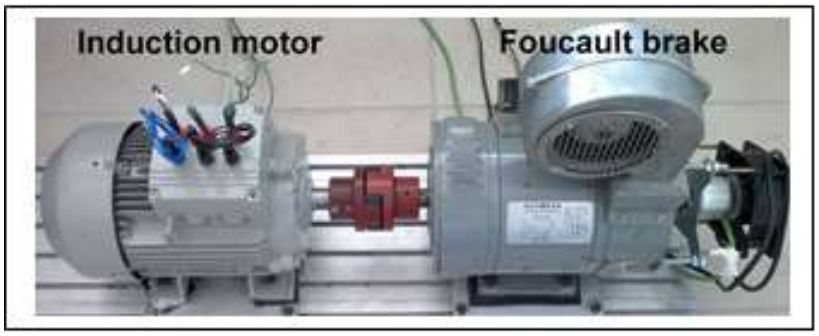

Figure 4. Experimental test rig

In the experimental study, Sinamics CU310DP inverter that has been used. The current, torque, and speed signals were recorded in computer from analogue output leads on the inverter for 10 secs with 10 kHz sampling frequency by means of Picoscope 4424, oscilloscope. The motor current has been recorded by means of current probe CA-60. Current probe has the features of carrying out measurement between a 0-60 A distance and giving output at 1 mV/10 mA and 1 mV/100 mA levels [23,24].

Table 2. Induction motor and brake parameters

Induction Motor			**Foucault Brake**	
Power	2.2 kw		Voltage	48 V DC
Frequency	50 Hz		Current	2.2 A
Voltage (Δ/Y)	220 /380 V		Speed	4000 rpm
Current(Δ/Y)	8.4 / 4.85 A		Torque	20 N.m
Speed	1420 rpm			
Power Factor	0.83			
Pair of poles (p)	2			

The current data measured for the healthy and faulty motors are recorded in Picoscope6 program and analysis of the data saved as text document can be easily carried out with the interface developed by the program of ‘’LabVIEW Sound and Vibration Assistant 2011’’. In the experimental study, an artificial broken rotor bar fault has been created in order to detect the faulty or broken rotor bars. Its aim is to see the difference between the healthy motor and the motor in which a fault has been created; and to detect the fault by examining the current data belonging to the faulty motor. Firstly, data for six different load conditions (0%, 25%, 50%, 75%, 100% and 115%) were collected from the healthy motor. There is a total of 28 bars in rotor. On one of the rotor bars, a hole of 17 mm was perforated by using a 6-mm-drill bit. Thus, a broken rotor bar was formed. Later, the motor was operated and

data for the 6 conditions were collected and recorded. Then the processes were repeated respectively for the conditions of 2 broken bars and 3 broken bars. The photos belonging to the faulty rotors that were created can be seen in Figure 5 [23,24].

MCSA is one of the most commonly used techniques used for detecting the faults of electrical motors. As a result of the analyses of healthy and faulty motors, it is clear that broken rotor bar cannot be detected when examining the changes in the current being attracted depending on time. Because the fault detection cannot be performed in time domain, the analyses in frequency domain are preferred.

Figure 5. Healthy and broken rotor bars

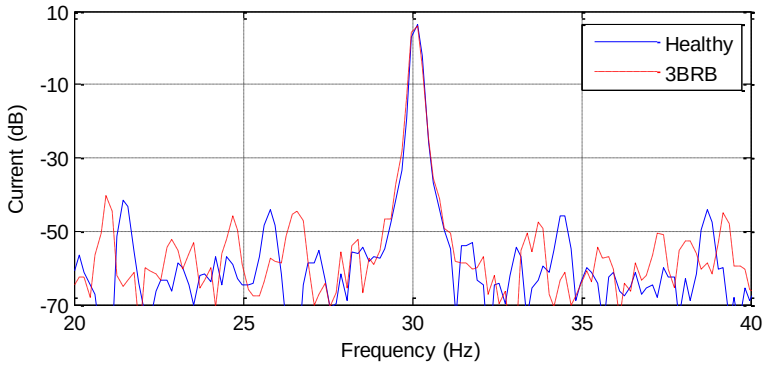

Figure 6. No-load operation for stationary 900 rpm (FFT)

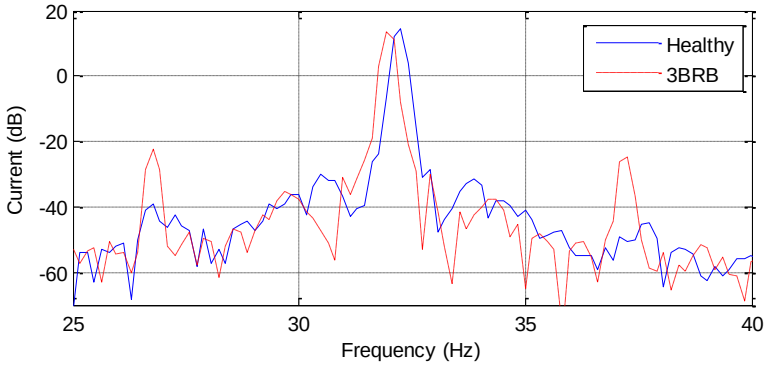

Figure 7. 100% load operation for stationary 900 rpm (FFT)

On Figure 6, amplitude values belonging to the motor currents obtained under the stationary operation conditions for 900 rpm are presented. In this graph, no-load operations of healthy motor and motor with three broken rotor bars were compared.

In this analysis which FFT was applied to, no sidebands belonging to the broken rotor bar were encountered as in literature. When the same study was conducted with 100% motor load, it will be observed in Figure 7 that sidebands that are symmetrical and can be calculated with Equation 1 occur at both sides of the operation frequency if the current amplitudes of the motor with three rotor bars are examined. It can be elicited from Figure 7 that lower sideband is in the frequencies of 27 Hz, and the upper sideband is in the frequencies of 37 Hz, and the change in their amplitudes is about 20 dB. In the same graph, it can also be observed that fundamental frequency shifted to 32 Hz even though speed is constant at 900 rpm. Its reason is that motor is driven by an inverter with closed speed control mode.

The graphs obtained after RB-OTA method was applied to the analyses under stationary and no-load 900 rpm operation conditions are presented in Figure 8. The place of any frequency component in order spectrum can be found with the expression of $Order = \frac{Frequency * 60}{n_r}$ where n_r is rotor speed. When the graphs are examined, it is obvious that the sidebands that the broken rotor bar fault has lead to are not seen as it is a no-load operation. None fault frequency components can be observed at the right and left sides of the 2nd order that corresponds to fundamental frequency.

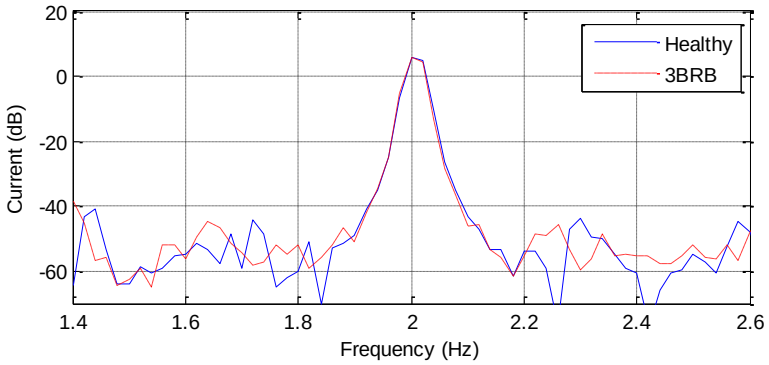

Figure 8. No-load operation for stationary 900 rpm (RB-OTA)

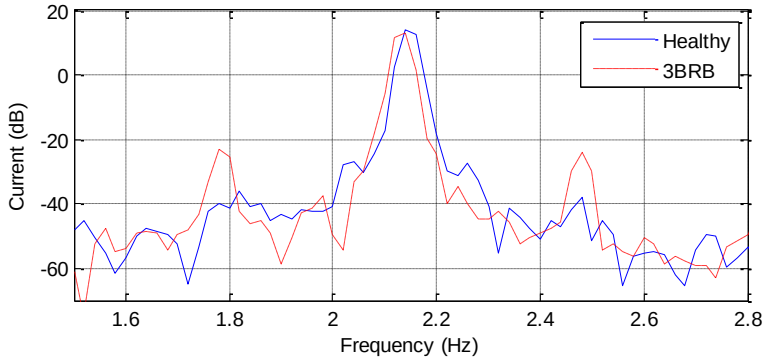

Figure 9. 100% load operation for stationary 900 rpm (RB-OTA)

When RB-OTA method was applied to motor current under stationary and full load 900 rpm operation conditions obtained results were presented in Figure 9. In the graph

belonging to the healthy motor, none fault frequency components can be observed at the right and left sides of the order 2.1 that corresponds to the fundamental frequency. Besides that, when the graph of the faulty motor is examined, it can be clearly seen that there are lower- and upper-sidebands at about orders of 1.78 and 2.48. As clearly seen from the graphs examined, fault detection cannot be performed no-load conditions, fault frequency components are observed in 100% load operation. Moreover, both FFT and RB-OTA methods enable the detection of the faults under stationary operation conditions [23].

The success of RB-OTA method comes out under non-stationary operation conditions. This method turns the non-stationary current signals into stationary condition by resampling them according to the dynamic speed signals.

Figure 10 and 11 are the graphs obtained after FFT was applied to the motor currents under dynamic 900 rpm. Figure 10 belongs to no-load operation condition while Figure 11 belongs to 100% load operation condition. When both graphs were examined, it is clear that fault detection cannot be performed under both load conditions. In Figure 11, 100% load operation, the component at 37 Hz frequency has occurred at the right side of the fundamental frequency as a result of the oscillation in speed.

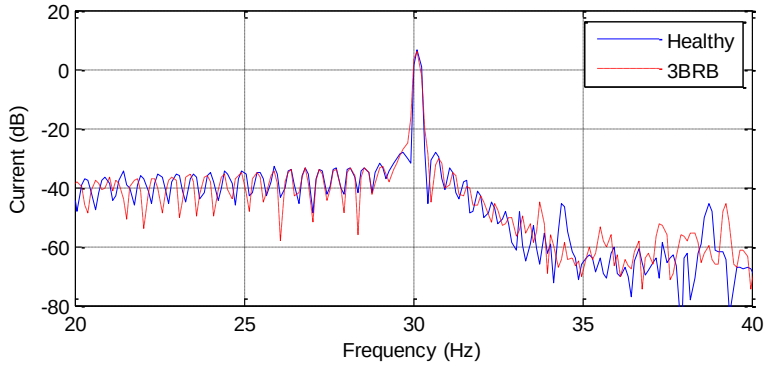

Figure 10. No-load operation for dynamic 900 rpm (FFT)

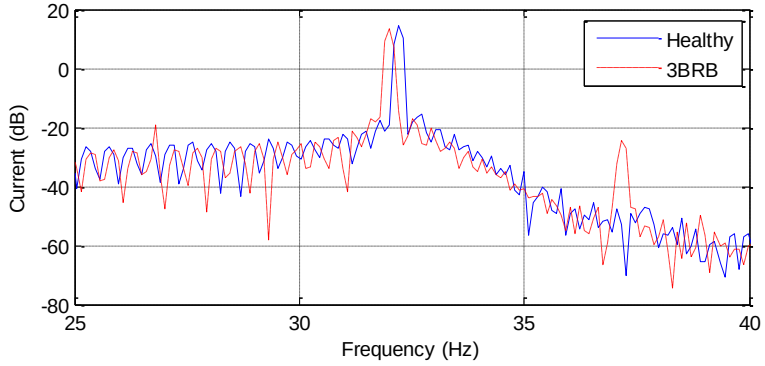

Figure 11. 100% load operation for dynamic 900 rpm (FFT)

Figure 12 contains the graphs obtained after RB-OTA method was applied to the motor currents under dynamic and no-load 900 rpm operation conditions. When the graphs belonging to the healthy and faulty motors are examined, it is observed that there is not a fault frequency component belonging to broken rotor bar at the right and lefts sides of order 2.

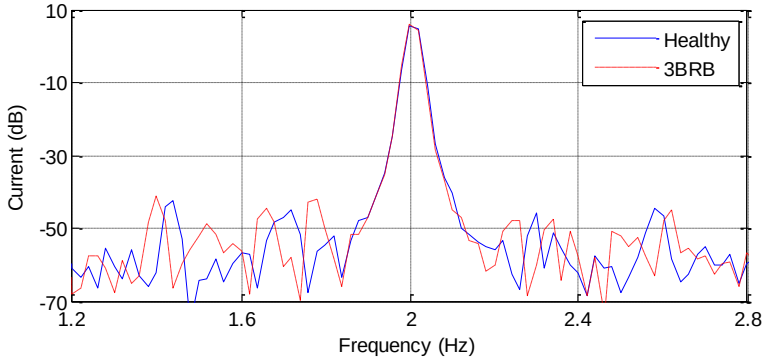

Figure 12. No-load operation for dynamic 900 rpm (RB-OTA)

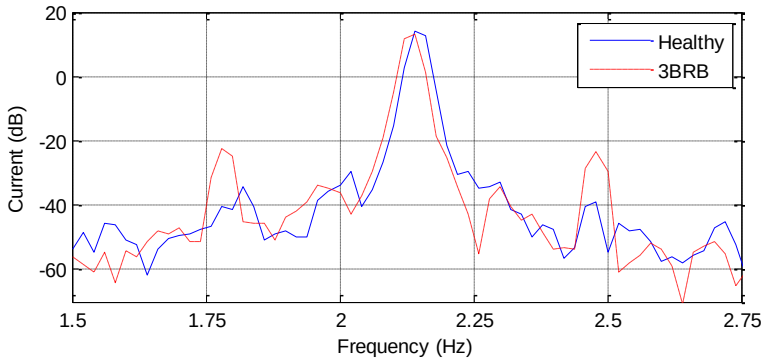

Figure 13. 100% load operation for dynamic 900 rpm (RB-OTA)

In Figure 13, it is observed that lower- and upper-sidebands belonging to the broken rotor bar fault occur at the orders of 1.78 and 2.48 and at equal distances from the order 2.14 that corresponds to the operation frequency. Amplitude values of the sidebands are about -38 dB in healthy motor while these values are about -22 dB in faulty motor. There is a rise of about 15 dB.

The change in the amplitude values of lower and upper sidebands order component according to the load and the number of faulty rotor bars has been given in Figure 14 and 15 respectively [23].

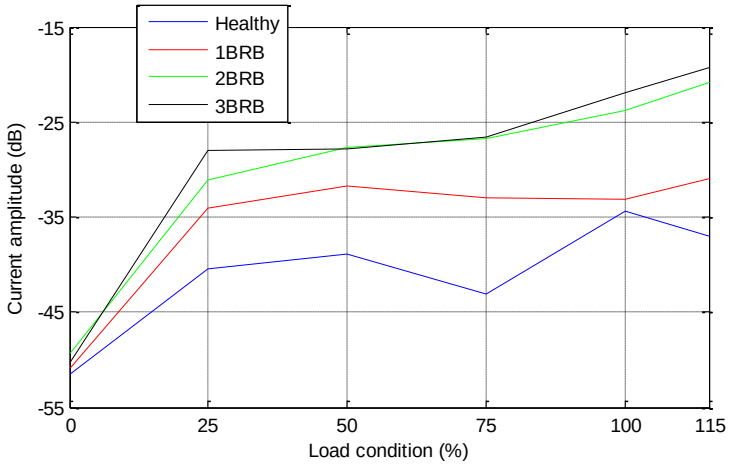

Figure 14. Amplitude values according to the dynamic 900 rpm load operation conditions (Lower-sideband fault frequency component)

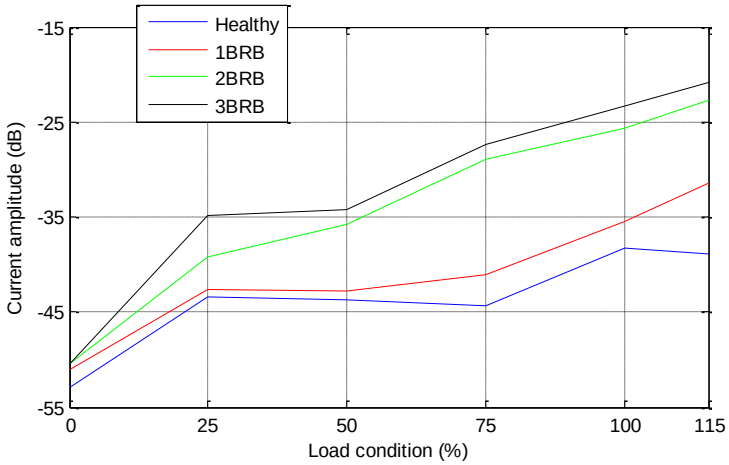

Figure 15. Amplitude values according to the dynamic 900 rpm load operation conditions (Upper-sideband fault frequency component)

Figure 14 contains fluctuations in the amplitude values of currents depending on the load condition for dynamic operation and for lower-sideband fault frequency components. The biggest amplitude change here is for three broken rotor bars. Similarly, Figure 15 is a graph that belongs to upper-sideband fault frequency component. The biggest amplitude change in this graph is also for three broken rotor bars with a rise of 20 dB. It is noticed that as the load condition of motor increases, amplitude fluctuation also increases [23].

In addition, the healthy and faulty (contains 3BRB) motors were operated according to the speed-time graph in Figure 16 and the analyzes were performed. Firstly, motor started to work at 1500 rpm and then it completed to work at 900 rpm. The analyzes was performed according to FFT and RB-OTA methods. Both methods were compared and the results obtained are presented in Figure 17 and 18 respectively.

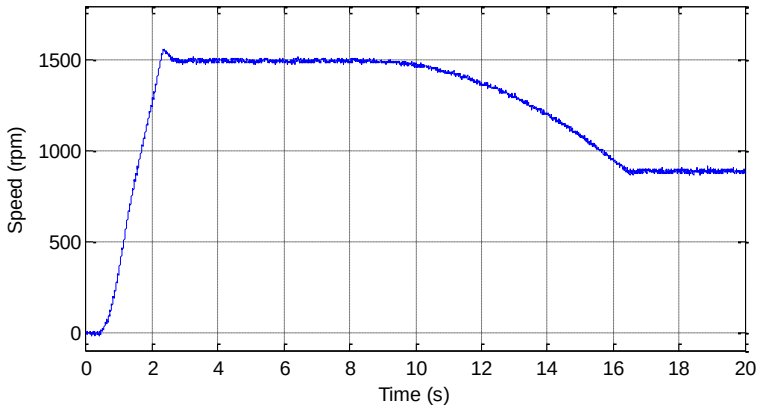

Figure 16. Dynamic operation condition speed-time graph

In Figure 17, It shows the comparison of the frequency spectrum for amplitude values belonging to motor current obtained in dynamic operation conditions and 100% load. When the graphs belonging to the healthy and faulty motors are examined, it is observed that there is not a fault frequency component belonging to broken rotor bar.

Figure 18 illustrates analysis results according to RB-OTA method. In Figure 18, it is observed that lower- and upper-sidebands belonging to the broken rotor bar fault occur in the orders of 1.92 and 2.45. Amplitude values of the sidebands in healthy motor are about -56 dB while these values are about -41 dB in the faulty motor.

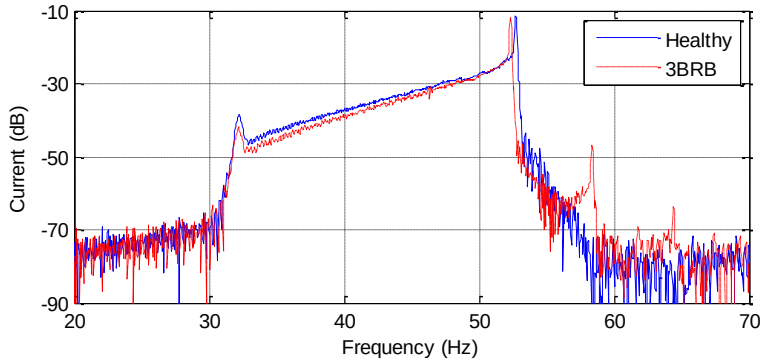

Figure 17. Amplitude spectrum for 100% load operation conditions and different speed (FFT)

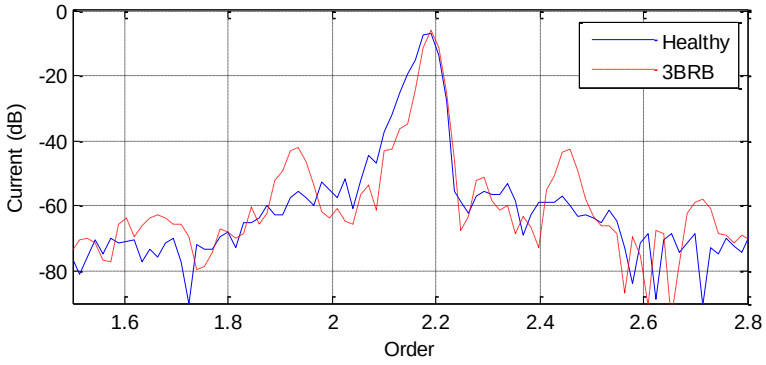

Figure 18. Amplitude spectrum for 100% load operation conditions and different speed (RB-OTA)

Conclusions

In this presented study, fault detection of the broken rotor bar in a three-phase squirrel cage induction motor has been performed experimentally. Depending on the stationary and non-stationary operation conditions of induction motor the analyses of the current signals were done with the FFT and RB-OTA methods.

FFT and RB-OTA methods at stationary operation at 900 rpm and full load condition yielded successful results. Rotor bar faults were detected with both methods.

It was observed that FFT method failed in the analyses carried out under non-stationary operation conditions and at the speed of 900. In this method, even though a frequency component occurs at the right side of the operation frequency depending on the speed oscillation, none fault-related frequency components occur at the left side.

Lower- and upper-sidebands fault frequency components belonging to the broken rotor bar fault were detected as a result of the analyses carried out under non-stationary operation conditions (900 rpm) with RB-OTA method.

References

[1] S. Nandi, H. A. Toliyat, X. Li, *Condition monitoring and fault diagnosis of electrical motors*, IEEE Transactions on Energy Conversion, Volume:20, Issue:4, pp:719-729, Dec. 2005.

[2] M. M. Tezcan, A. I. Çanakoğlu, *Finite element study of induction motorshaving broken rotor bar faults*, 5. International Advanced Technologies Symposium, Karabük, 2009.

[3] I. Aydın, *The using of data mining and soft computing techniques in fault diagnosis*, Fırat University Graduate School of Naturel and Applied Sciences, Master thesis, 2006.

[4] M. L. Sin, W. L. Soong, N. Ertuğrul, *Induction machine on-line condition monitoring and fault diagnosis*, University of Adelaide, 2003.

[5] C. C. Yeh, A. S. Ahmed, R. J. Povinelli, D. M. Ionel, *A reconfigurable motor for experimental emulation of stator winding interturn and broken bar faults in polyphase induction machine,* IEEE Transactions on Energy Conversion, Volume: 23, Issue:4, Dec. 2008.

[6] M. Akar, *Detection of rotor bar faults in field oriented controlled induction motors*, Journal of Power Electronics, Volume:12, Issue:6, pp:982-991, Nov. 2012.

[7] M. Akar , *Mechanical fault diagnosis in the permanent magnet synchronos motor with artifical intelligence techniques*, Sakarya University Institute of Science, PhD. Thesis, Sakarya, 2009.

[8] H. Arabacı, O. Bilgin, *Detection of rotor bar faults by using stator current envelope*, Proceedings of the World Congress on Engineering 2011, Volume:II, pp:1432-1435, London, U.K, 2011.

[9] S. Chen, *Induction machine broken rotor bar diagnostics using prony analysis*, School of Electrical & Electronic Engineering, University of Adelaide, Master's Thesis, Adelaide, Australia, 2008.

[10] R. Supangat, *Online condition monitoring and detection of stator and rotor faults in induction motors*, University of Adelaide, PhD Thesis, Adelaide, Australia, 2008.

[11] N. Mehala, R. Dahiya, *Rotor faults detection in induction motor by wavelet analysis*, International Journal of Engineering Science and Technology, Volume:1, Issue:3, pp:90-99, 2009.

[12] C. Costa, M. Kashiwagi, M. H. Mathias, *Rotor failure detection of induction motors by wavelet transform and Fourier transform in non-stationary condition*, Case Studies in Mechanical Systems and Signal Processing, Volume:1, pp:15–26, 2015.

[13] M. Bayrak, A. Küçüker, *A power based algorithm design for detection of broken rotor bars faults in three phase induction motors*, Journal of the Faculty of Engineering and Architecture of Gazi University, Volume:21, Issue:2, pp:303-311, 2016.

[14] M. Akar, İ. Çankaya, *Broken rotor bar fault detection in inverter-fed squirrel cage induction motors using stator current analysis and fuzzy logic*, Turk J Elec. Eng & Comp. Sci, Volume:20, Issue:1, 2012.

[15] P. Shi, Z. Chen, Y. Vagapov, Z. Zouaoui, *A new diagnosis of broken rotor bar fault extent in three phase squirrel cage induction motor*, Mechanical Systems and Signal Processing, Volume:42, pp:388-403, 2014.

[16] V. Ghorbanian, J. Faiz, *A survey on time and frequency characteristics of induction motors with broken rotor bars in line-start and inverter-fed modes*, Mechanical Systems and Signal Processing, Volume:54-55, pp:427-456, 2015.

[17] M. O. Mustafa, G. Nikolakopoulos, T. Gustafsson, D. Kominiak, *A fault detection scheme based on minimum identified uncertainty bounds violation for broken rotor bars in induction motors*, Control Engineering Practice, Volume:48, pp:63-77, 2016.

[18] S. Ergin, A. Uzuntaş, M. B. Gülmezoğlu, *Detection of stator, bearing and rotor faults in induction motors*, Procedia Engineering Volume:30,pp:1103 – 1109, 2012.

[19] M. G. Armaki ,R. Roshanfekr, *A new approach for fault detection of broken rotor bars in induction motor based on support vector machine*, Proceedings of ICEE (Electrical Engineering), 18th Iranian Conference on , May 2010.

[20] G. B. Kliman, R.A. Koegl, J. Stein, R.D. Endicott, M.W. Madden, *Noninvasive detection of broken rotor bars in operating induction motors*, IEEE Transactions on Energy Conversion, Volume:3, Issue:4, pp:873–879, 1988.

[21] K. Wang, *Vibration monitoring on electrical machine using vold-kalman filter order tracking*, Master's Thesis, Mechanical and Aeronautical Engineering, University of Pretoria, 2008.

[22] J. R. Blough, *Adaptive resampling-transforming from the time to the angle domain*, IMAC-XXIV:Conference & Exposition on Structural Dynamics, 2006.

[23] T. Doğruer, *The detection of rotor bar broken fault in asynchronous motor drived by inverter*, Gaziosmanpaşa University Graduate School of Naturel and Applied Sciences, Master's Thesis, 2012.

[24] T. Doğruer, M. Akar, *İndüksiyon motorlarında durağan olmayan çalışma şartlarında kırık rotor çubuğu arızasının tespiti*, EEB2016 Elektrik-Elektronik ve Bilgisayar Sempozyumu, Tokat, Mayıs 2016.